Materials Science & Engineering A 565 (2013) 392–395

Contents lists available at SciVerse ScienceDirect

Materials Science & Engineering A

journal homepage: www.elsevier.com/locate/msea

Evaluations of stress-free lattice spacings and residual stresses in a quenched carbon steel cylinder using neutron diffraction

Minsu Jung [a,1], Mihyun Kang [a,b], Wanchuck Woo [b], Young-Kook Lee [a,*]

[a] Department of Materials Science and Engineering, Yonsei University, Seoul 120-749, Korea
[b] Neutron Science Division, Korea Atomic Energy Research Institute, Daejeon 305-353, Korea

ARTICLE INFO

Article history:
Received 18 September 2012
Received in revised form
28 December 2012
Accepted 29 December 2012
Available online 4 January 2013

Keywords:
Neutron diffraction
Residual stresses
Microstructure
Stress-free lattice spacing
Steel
Quenching

ABSTRACT

Microstructure-dependent stress-free lattice spacings (d_0) were measured using neutron diffraction in a comb-like specimen fabricated from a quenched carbon steel cylinder. The d_0 values increased with cylinder radius due to the increase in the martensite (α') fraction with the radius and were comparable to d_0 values calculated using the lattice parameter of each phase, taking the auto-tempering effect into consideration. Using the measured d_0 values, we suggested a relationship between the d_0 and α' fraction and evaluated macroscopic residual stresses in the quenched steel cylinder.

1. Introduction

Macroscopic residual stresses can be introduced into mechanical components during various thermal or thermomechanical processes such as heat treatment, forming, and welding [1–4]. Accurate evaluation of residual stresses is important because they play a crucial role in performance, integrity, and lifetime of the components [2,3]. Accordingly, various techniques for measuring residual stresses have been developed, such as X-ray and neutron diffractions, ultrasonic velocity, hole drilling, and layer removal techniques[4]. Of these methods, neutron diffraction has been extensively used for measuring residual stresses inside the components owing to the deep and non-destructive penetration of neutrons up to several centimeters into most metals and alloys [5–14].

For the determination of macroscopic residual stresses by neutron diffraction, it is important to accurately measure the stress-free lattice spacing (d_0) of a sample because residual stresses are obtained using the difference between the d_0 and the stressed lattice spacing (d). As the d_0 is significantly influenced by microstructure, it is necessary to acquire microstructure-dependent d_0 values at the same locations where residual stresses would be evaluated. If stress-free specimens with different microstructures are taken from various locations in a sample, the microstructure-dependent d_0 values can be directly measured using neutron diffraction [15]. For example, the d_0 values of various steel welds have been directly measured by neutron diffraction using stress-free cubes [12] or combs [13,14] that were taken from the welds.

Unlike studies conducted on steel welds, neutron diffraction studies on residual stresses in quenched steels have been performed mostly with transformation-free quenched steels such as austenitic stainless steels [10,11] or carbon steels quenched from a temperature below the austenite start temperature (A_{c1}) [9]. For a quenched carbon steel involving phase transformations, microstructure-dependent d_0 values have been indirectly obtained using a predeterminate relationship between the d_0 and the martensite (α') fraction and calculated α' fractions at given locations in the quenched sample [16]. To date, there are few direct measurements of the microstructure-dependent d_0 values by neutron diffraction and their assessments in quenched carbon steels with inhomogeneous microstructures.

Therefore, in the present study, we tried to directly measure using neutron diffraction the microstructure-dependent d_0 values at various locations in a stress-free comb-like specimen fabricated from a carbon steel cylinder quenched from 900 °C. In addition, we evaluated the measured d_0 values by comparing them with theoretically calculated values. The theoretical d_0 values were calculated using phase fractions and the lattice parameters of

* Corresponding author. Tel.: +82 2 2123 2831; fax: +82 2 312 5375.
E-mail address: yklee@yonsei.ac.kr (Y.-K. Lee).
[1] Current address: Max Planck Institute for Intelligent Systems (formerly Max Planck Institute for Metal Research), Heisenbergstrasse 3, 70569 Stuttgart, Germany.

0921-5093/$ - see front matter © 2013 Elsevier B.V. All rights reserved.
http://dx.doi.org/10.1016/j.msea.2012.12.075

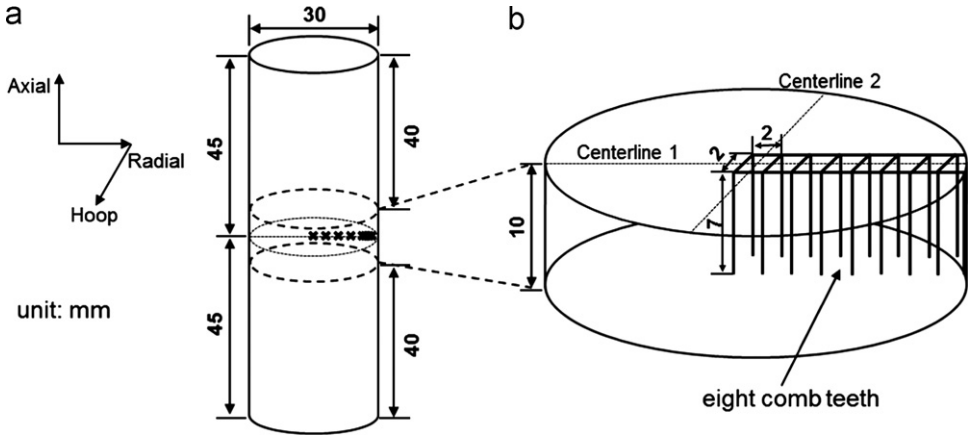

Fig. 1. Schematic diagrams of (a) the locations (x) for neutron diffraction measurements in a quenched S45C steel cylinder and (b) a stress-free comb-like specimen fabricated from the quenched steel sample.

ferrite (α) and α', considering the auto-tempering effect in the quenched steel cylinder. Finally, macroscopic residual stresses in the quenched steel cylinder with an inhomogeneous microstructure were determined using the measured d_0 and d values.

2. Experimental procedure

A commercial medium-carbon steel (S45C) with the chemical composition Fe-0.45C-0.70Mn-0.29Si by weight percent was used in the present study. A round bar measuring 38 mm in diameter and 900 mm in length was provided by SeAHBesteel Corp. A cylinder of 30 mm diameter and 90 mm length was machined from the round bar for a quenching test (Fig. 1(a)). The cylindrical specimen was austenitized at 900 °C for 15 min and then quenched in water at room temperature. The quenched steel cylinder possessed a mixed microstructure of α, pearlite (α+cementite (θ)), bainite ($\alpha+\theta$), and α', depending on the location [17].

Neutron diffraction measurements were performed using a residual stress instrument at HANARO, Korea Atomic Energy Research Institute (KAERI). Fig. 1(a) shows the locations for neutron diffraction measurements in the quenched S45C steel cylinder (radius (r)=0.0, 3.0, 6.0, 9.0, 12.0, 12.5, 13.0, and 13.5 mm). A Si (220) monochromatic neutron beam with a wavelength of 2.3845 Å was employed, and the scattering volume was 1 (radial) × 4 (axial) × 1 (hoop) mm^3. The diffraction peaks of the {110} plane were measured in the radial, axial, and hoop directions at given radii of the quenched steel cylinder, and d values were converted from the position of the diffraction peaks by Bragg's law. After the measurement of d values, a macroscopic stress-free comb-like specimen was prepared from the quenched steel cylinder using an electro-discharge machine [15], as shown in Fig. 1(b). The dimensions of each comb tooth was 2 (radial) × 7 (axial) × 2 (hoop) mm^3. Microstructure-dependent d_0 values were determined from the diffraction peaks measured at eight teeth of the stress-free comb-like specimen.

Lattice strains (ε_i) were calculated from the measured d_0 and d values using the following equation: ε_i (Å)=$(d-d_0)/d_0$. Residual stresses (σ_i) in the radial (R), axial (A), and hoop (H) directions were calculated using the generalized Hooke's law:

$$\sigma_i = \frac{E}{1+v}\left\{\varepsilon_i + \frac{v}{1\text{-}2v}(\varepsilon_R+\varepsilon_A+\varepsilon_H)\right\},\ i=(R, A, H) \quad (1)$$

where the subscript i refers to the directional components of strain and stress, E is the Young's modulus, and v is Poisson's ratio. Values of E (=210.5 GPa) and v (=0.25) for the ⟨110⟩ direction of the ferritic iron were used in the calculations [15].

3. Results and discussion

3.1. Diffraction peaks in the stress-free specimen

Fig. 2(a) shows the raw neutron diffraction data of α {110} and α' {110} planes and the Gaussian curves fit to the data, which were collected along the hoop direction at a radius of 6 mm in the stress-free comb-like specimen shown in Fig. 1(b). Although α has a bcc structure and α' has a bct structure, a small difference in lattice spacing between the α and α' phases in S45C steel (<0.02 Å, or a difference in diffraction angle of $<0.7°$) causes their diffraction peaks to be indistinguishable and overlapped, as shown in Fig. 2(a). The differences in lattice spacing between α {110} and α' (101)/(011) and between α {110} and α' (110) are 0.016 Å and 0.0042 Å, respectively, and the corresponding differences in diffraction angles are 0.65° and 0.17°, respectively.

Fig. 2(b) shows Gaussian curves fit to neutron diffraction peaks measured along the hoop direction at various radii in the stress-free comb-like specimen. It is interesting to note that the diffraction peak was broadened and shifted toward smaller diffraction angles with increasing radius. This broadening is most likely due to the increase in the α' fraction and plastic deformation by thermal stress with increasing radius [17]. The effects of increased α' fraction and plastic deformation on the broadening and shifting of diffraction peaks can be explained as follows. The diffraction peaks of α' (101) and (011) planes appear at smaller diffraction angles than that of the α {110} plane, whereas the diffraction peak of the α' (110) plane appears at a larger angle, resulting in peak broadening. The difference in diffraction angle between α' (101) and (011) planes and the α {110} plane is larger than that between the α' (110) and α {110} planes. The total diffraction intensity of α' (101) and (011) planes is stochastically twice as high as that of the α' (110) plane. These differences cause the observed peak shifting. Thus, the mixed diffraction peak of α {110} and α' {110} planes is broadened and shifted to a lower diffraction angle with increased α' fraction. The increase in crystal defects such as dislocations and vacancies introduced by the martensitic transformation and plastic deformation also contributes to the observed peak broadening [18].

3.2. Stress-free and stressed lattice spacings

To acquire more reliable d_0 values, diffraction peaks were additionally measured along the radial and axial directions, as well as the above-mentioned hoop direction. The average d_0 values were obtained from the diffraction peaks and are plotted against the radius in Fig. 3(a). The measured d_0 value increased